# Large electric-field-induced strain in centrosymmetric crystals of a dipolar ruthenium alkynyl complex

*Kenny Lau, Adam Barlow, Graeme J. Moxey, Qian Li, Yun Liu*, Mark G. Humphrey*, Marie P. Cifuentes, Terry Frankcombe and Rob Stranger*

Research School of Chemistry, Australian National University, ACT 2601, Australia

**Synthetic Procedures.** Complexes **1**,[1] **2**,[1] and **3**[1] have been reported previously, but were synthesized by different procedures to those in the literature in the present work, as outlined below. Their identities were confirmed by comparison of $^{1}H$, $^{31}P$ and $^{13}C$ NMR spectral data with literature values,[1] in addition to single-crystal X-ray diffraction studies. All reactions were performed under a nitrogen atmosphere with the use of Schlenk techniques unless otherwise stated. $CH_2Cl_2$ was dried by distilling over calcium hydride. "Petrol" refers to a fraction of boiling range 60-80 °C. *trans*-$[RuCl_2(dppe)_2]$,[2] $[RuCl(dppe)_2]PF_6$,[2] and 4-nitrophenylacetylene[3] were synthesized by literature procedures. All other reagents were used as received.

**Synthesis of *trans*-[Ru(C≡CC$_6$H$_4$-4-NO$_2$)(C≡CPh)(dppe)$_2$] (1).** *trans*-[Ru(C≡CC$_6$H$_4$-4-NO$_2$)Cl(dppe)$_2$] (**2**) (0.500 g, 0.460 mmol), $NaPF_6$ (0.120 g, 0.714 mmol) and phenylacetylene (0.070 g, 0.470 mmol) were added to distilled $CH_2Cl_2$ (25 mL). The resultant mixture was stirred for 5 min, triethylamine (0.2 mL) was added, and the mixture was stirred overnight and then added to petrol (150 mL), affording a precipitate that was

collected by filtration and washed with methanol. A $CH_2Cl_2$ extract of the red solid was passed through a short pad of alumina, eluting with 2:1:0.1 $CH_2Cl_2$/petrol/triethylamine. The eluate was reduced in volume to give *trans*-[Ru(C≡C$C_6H_4$-4-$NO_2$)(C≡CPh)$(dppe)_2$] (0.420 g, 79 %) as a bright red solid.[1] Crystals of **1** suitable for a single-crystal X-ray diffraction study and employed in the PFM and BE-SSPFM studies were grown by slow evaporation of a $CHCl_3$ solution. A polymorph, **1a**, was obtained by slow diffusion of methanol into a $CH_2Cl_2$ solution (see X-ray Crystallographic Studies), although this was not used in the PFM and BE-SSPFM studies.

**Synthesis of *trans*-[Ru(C≡C$C_6H_4$-4-$NO_2$)Cl$(dppe)_2$] (2).** [RuCl$(dppe)_2$]$PF_6$ (0.710 g, 0.658 mmol) and 4-nitrophenylacetylene (0.120 g, 0.816 mmol) were added to distilled $CH_2Cl_2$ (30 mL). The resultant mixture was stirred for 3 h and then added to petrol (150 mL), affording a precipitate that was collected by filtration. The solid was added to a mixture of $CH_2Cl_2$ and triethylamine (10:1, 15 mL), and the mixture was stirred for 10 min and then passed through a short pad of alumina, eluting the red-colored band with 2:1:0.1 $CH_2Cl_2$/petrol /triethylamine. The eluate was reduced in volume to give *trans*-[Ru(C≡C$C_6H_4$-4-$NO_2$)Cl$(dppe)_2$] (**2**) as a red solid (0.54 g, 77%). Crystals of **2** suitable for a single-crystal X-ray diffraction study and employed in the PFM and BE-SSPFM studies were grown by slow diffusion of petrol into a solution of **2** in $CH_2Cl_2$. Several polymorphs of **2** were also obtained, by varying the crystallization solvents and conditions (**2a**, **2b**, and a previously published structure **2**.$CH_2Cl_2$[4]: see X-ray Crystallographic Studies), but these were not used in the PFM and BE-SSPFM studies.

**Synthesis of *trans*-[Ru(C≡CPh)$_2$$(dppe)_2$] (3).** *trans*-[$RuCl_2(dppe)_2$] (0.530 g, 0.539 mmol) and $NaPF_6$ (0.190 g, 1.13 mmol) were added to distilled $CH_2Cl_2$ (25 mL). The resultant

mixture was stirred for 3 h, phenylacetylene (0.13 mL, 1.18 mmol) was added, and the mixture was stirred for a further 5 min. Triethylamine (0.2 mL) was then added, and the mixture stirred for 1 h and then added to petrol (100 mL). The resulting precipitate was collected by filtration and washed with methanol (50 mL), to yield *trans*-[Ru(C≡CPh)$_2$(dppe)$_2$] (**3**) (0.47 g, 78 %) as a pale yellow solid. Crystals of **3** suitable for a single-crystal X-ray diffraction study (unit cell only) and employed in the PFM and BE-SSPFM studies were obtained by slow diffusion of petrol into a solution of **3** in $CH_2Cl_2$. The unit cell data were in agreement with literature values.[5]

**X-ray Crystallographic Studies.** *General Procedures.* Intensity data were collected using an Enraf-Nonius KAPPA CCD diffractometer at 200 K using graphite-monochromated Mo$K_\alpha$ radiation ($\lambda$ = 0.7170 Å). Suitable crystals were immersed in viscous hydrocarbon oil and mounted on glass fibers which were mounted on the diffractometer. Using $\psi$ and $\omega$ scans, $N_t$ (total) reflections were measured, which were reduced to $N_o$ unique reflections, with $F_o > 2\sigma(F_o)$ being considered "observed". Data were initially processed and corrected for absorption using the programs DENZO[6] and SORTAV.[7] The structures were solved using direct methods, and observed reflections were used in least-squares refinement on $F^2$, with anisotropic thermal parameters refined for non-hydrogen atoms. Hydrogen atoms were constrained in calculated positions and refined with a riding model. Structure solutions and refinements were performed using the programs SHELXS-97 and SHELXL-97[8] through the graphical interface Olex2,[9] which was also used to generate the figures. CCDC: 988100 – 988103 (**1**, **2**, **2a**, **2b**) and 997325 (**1a**) contain the supplementary crystallographic data for this paper. These data can be obtained free of charge from The Cambridge Crystallographic Data Centre via www.ccdc.cam.ac.uk/data_request/cif.

Crystal data for **1**: $C_{68}H_{56}NO_2P_4Ru$, $M$ = 1144.09, orange plate, 0.13 × 0.10 × 0.03 mm$^3$, triclinic, space group $P$-1 (No. 2), $a$ = 9.4345(19), $b$ = 12.947(3), $c$ = 13.486(3) Å, $\alpha$ = 116.68(3), $\beta$ = 95.93(3), $\gamma$ = 103.41(3)°, $V$ = 1390.3(5) Å$^3$, $Z$ = 1, $D_c$ = 1.366 g/cm$^3$, $F_{000}$ = 591, $2\theta_{max}$ = 55.0º, $\mu$ = 0.445 mm$^{-1}$, 24109 reflections collected, 6204 unique ($R_{int}$ = 0.1170). Final *GooF* = 1.050, *R1* = 0.0627, *wR2* = 0.0879, *R* indices based on 3384 reflections with I > 2σ(I) (refinement on $F^2$), 358 parameters, 0 restraints. Crystals of **1a** were grown from slow diffusion of methanol into a $CH_2Cl_2$ solution. Crystal data for **1a**: $C_{68}H_{56}NO_2P_4Ru$, $M$ = 1144.09, orange needle, 0.09 × 0.04 × 0.03 mm$^3$, triclinic, space group $P$-1 (No. 2), $a$ = 9.3858(19), $b$ = 13.093(3), $c$ = 13.858(3) Å, $\alpha$ = 96.07(3), $\beta$ = 108.44(3), $\gamma$ = 93.38(3)°, $V$ = 1598.8(6) Å$^3$, $Z$ = 1, $D_c$ = 1.188 g/cm$^3$, $F_{000}$ = 591, $2\theta_{max}$ = 45.5º, $\mu$ = 0.387 mm$^{-1}$, 3985 reflections collected, 3985 unique ($R_{int}$ = 0.1250). Final *GooF* = 1.036, *R1* = 0.1012, *wR2* = 0.2362, *R* indices based on 2403 reflections with I > 2σ(I) (refinement on $F^2$), 310 parameters, 2 restraints. **Variata**. In **1** and **1a**, the nitro substituent is disordered over the two 4-phenylethynyl sites, occupancy 0.5:0.5, and analogous to the structural study of the dppm [bis(diphenylphosphino)methane] analogue *trans*-[Ru(C≡C$C_6H_4$-4-$NO_2$)(C≡CPh)$(dppm)_2$] for which the ruthenium atom also sits on a crystallographic inversion center.[10] For **1a**, the crystal diffracted extremely weakly ($\theta_{max}$ 22.72°), even with long exposure times. The best available crystal was chosen for the data collection, and the data were collected at low temperature to enhance the reflection intensities. For **1a**, bond geometry restraints were applied to atoms N1, O1 and O2 of the 4-nitrophenylalkynyl ligand. Anisotropic displacement parameter restraints were applied to atoms C3 - C8 and N1, O1 and O2 of the 4-nitrophenylalkynyl ligand. For **1a**, a lattice dichloromethane molecule could not be successfully modelled, and was therefore removed from the refinement using Platon SQUEEZE.[11]

Crystal data for **2**: $C_{61.50}H_{55}Cl_4NO_2P_4Ru$ (**2**.1.5$CH_2Cl_2$), $M$ = 1206.81, red plate, 0.12 × 0.10 × 0.03 mm$^3$, triclinic, space group $P$-1 (No. 2), $a$ = 9.2824(19), $b$ = 12.920(3), $c$ = 23.719(5) Å, $\alpha$ = 94.68(3), $\beta$ = 94.17(3), $\gamma$ = 99.15(3)°, $V$ = 2788.4(10) Å$^3$, $Z$ = 2, $D_c$ = 1.437 g/cm$^3$, $F_{000}$ = 1238, 2$\theta_{max}$ = 55.7º, $\mu$ = 0.632 mm$^{-1}$, 56586 reflections collected, 13209 unique ($R_{int}$ = 0.0506). Final *GooF* = 1.034, *R1* = 0.0425, *wR2* = 0.1118, *R* indices based on 10297 reflections with I > 2σ(I) (refinement on $F^2$), 667 parameters, 1 restraint. Crystals of **2a** were grown from slow diffusion of petrol into a $CH_2Cl_2$ solution. Crystal data for **2a**: $C_{60}H_{52}ClNO_2P_4Ru$, $M$ = 1079.43, orange block, 0.10 × 0.08 × 0.08 mm$^3$, triclinic, space group $P$-1 (No. 2), $a$ = 9.4558(19), $b$ = 12.924(3), $c$ = 13.619(3) Å, $\alpha$ = 117.44(3), $\beta$ = 95.49(3), $\gamma$ = 103.91(3)°, $V$ = 1392.0(5) Å$^3$, $Z$ = 1, $D_c$ = 1.288 g/cm$^3$, $F_{000}$ = 556, 2$\theta_{max}$ = 55.0º, $\mu$ = 0.486 mm$^{-1}$, 6366 reflections collected, 6366 unique ($R_{int}$ = 0.0474). Final *GooF* = 1.559, *R1* = 0.1030, *wR2* = 0.3303, *R* indices based on 5265 reflections with I > 2σ(I) (refinement on $F^2$), 313 parameters, 36 restraints. Crystals of **2b** were grown from slow diffusion of hexane into a $CH_2Cl_2$ solution. Crystal data for **2b**: $C_{63}H_{59}ClNO_2P_4Ru$ (**2b**.0.5$C_6H_{14}$), $M$ = 1122.51, red block, 0.12 × 0.10 × 0.08 mm$^3$, triclinic, space group $P$-1 (No. 2), $a$ = 10.028(2), $b$ = 12.594(3), $c$ = 22.413(5) Å, $\alpha$ = 93.19(3), $\beta$ = 91.02(3), $\gamma$ = 108.48(3)°, $V$ = 2678.7(9) Å$^3$, $Z$ = 2, $D_c$ = 1.392 g/cm$^3$, $F_{000}$ = 1162, 2$\theta_{max}$ = 57.4º, $\mu$ = 0.508 mm$^{-1}$, 61726 reflections collected, 13697 unique ($R_{int}$ = 0.0381). Final *GooF* = 1.019, *R1* = 0.0322, *wR2* = 0.0770, *R* indices based on 11515 reflections with I > 2σ(I) (refinement on $F^2$), 650 parameters, 0 restraints.

**Variata:** For **2**, bond geometry restraints were applied to atoms C62 and Cl4 of the lattice dichloromethane molecule. For **2a,** the chloride and 4-nitrophenylethynyl ligands are disordered by symmetry over two positions, occupancy 0.5:0.5. Restraints were applied to the anisotropic displacement parameters of all atoms on the 4-nitrophenylethynyl and chloride

ligands. In addition, bond geometry restraints were applied to atoms N1, O1 and O2, and the phenyl ring C3-C8.

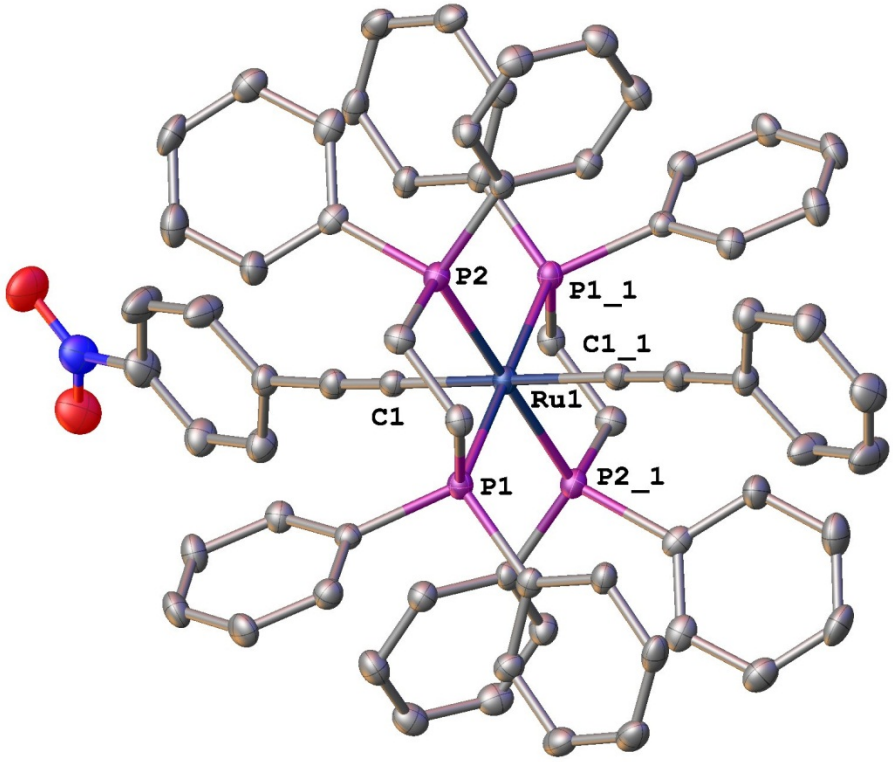

Figure S1. ORTEP plot and atom numbering scheme for *trans*-[Ru(C≡C$C_6H_4$-4-$NO_2$)(C≡CPh)$(dppe)_2$] **(1)**, with thermal ellipsoids set at the 30% probability level. Hydrogen atoms and the disordered nitro substituent are omitted for clarity. Selected bond lengths (Å) and angles (°) for **1**: Ru(1)-C(1) 2.072(4), Ru(1)-P(2)_1 2.3549(13), Ru(1)-P(1) 2.3588(14), C(1)-Ru(1)-C(1)_1 180.000(2), C(1)-Ru(1)-P(2)_1 88.16(11), C(1)-Ru(1)-P(2) 91.84(11), P(2)_1-Ru(1)-P(2) 180.000(1), C(1)-Ru(1)-P(1) 99.36(12), C(1)_1-Ru(1)-P(1) 80.64(12), P(2)_1-Ru(1)-P(1) 97.05(5), P(2)-Ru(1)-P(1) 82.95(5), P(1)-Ru(1)-P(1)_1 180.00(5). Symmetry operation used to generate equivalent atoms: _1 -x+1,-y+1,-z+2.

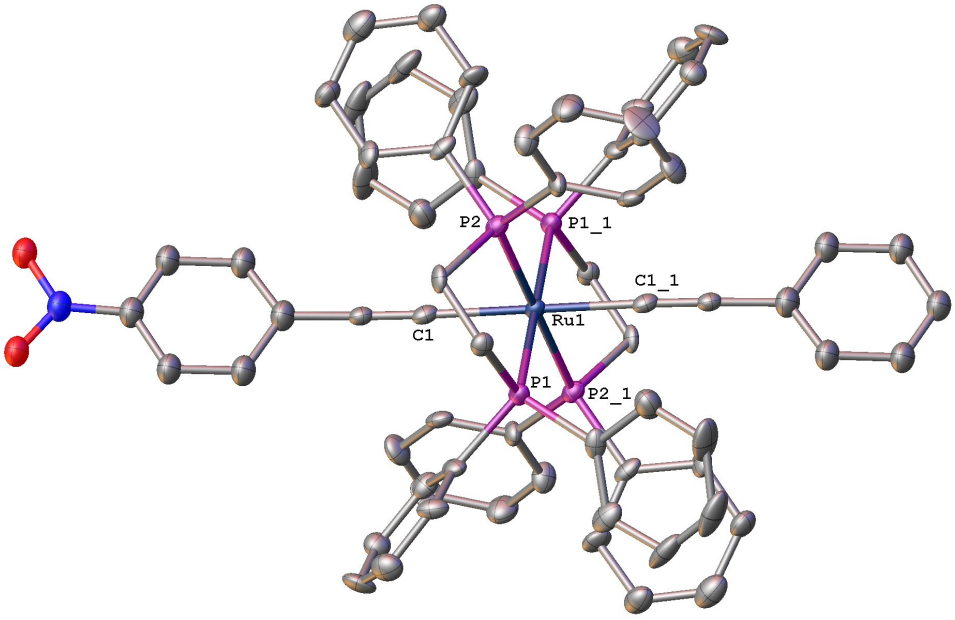


Figure S2. ORTEP plot and atom numbering scheme for *trans*-[Ru(C≡C$C_6H_4$-4-$NO_2$)(C≡CPh)$(dppe)_2$] **(1a)**, with thermal ellipsoids set at the 30% probability level. Hydrogen atoms and the disordered nitro substituent are omitted for clarity. Selected bond

lengths (Å) and angles (°) for **1**: Ru(1)-C(1) 2.064(12), Ru(1)-P(2)_1 2.366(3), Ru(1)-P(1) 2.359(3), C(1)-Ru(1)-C(1)_1 180.000(3), C(1)-Ru(1)-P(2)_1 98.5(3), C(1)-Ru(1)-P(2) 81.5(3), P(2)_1-Ru(1)-P(2) 180.000(1), C(1)-Ru(1)-P(1) 87.7(3), C(1)_1-Ru(1)-P(1) 92.3(3), P(2)_1-Ru(1)-P(1) 96.88(10), P(2)-Ru(1)-P(1) 83.12(10), P(1)-Ru(1)-P(1)_1 180.000(1). Symmetry operation used to generate equivalent atoms: _1 -x,-y+2,-z+1.

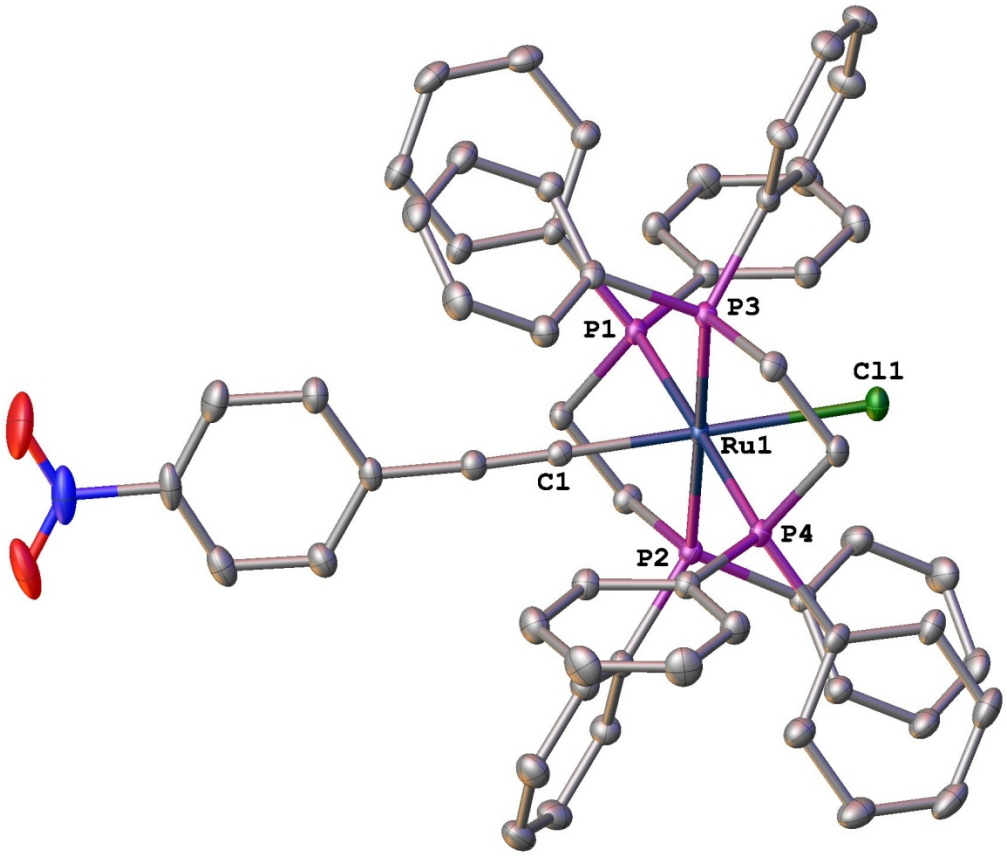


Figure S3. ORTEP plot and atom numbering scheme for *trans*-[Ru(C≡C$C_6H_4$-4-$NO_2$)Cl(dppe)$_2$] **(2)**, with thermal ellipsoids set at the 30% probability level. Hydrogen atoms and lattice dichloromethane molecules are omitted for clarity. Selected bond lengths (Å) and angles (°) for **2**: Ru(1)-C(1) 1.984(3), Ru(1)-P(2) 2.3632(9), Ru(1)-P(3) 2.3687(9), Ru(1)-P(4) 2.3862(12), Ru(1)-P(1) 2.3881(12), Ru(1)-Cl(1) 2.5084(10), C(1)-Ru(1)-P(2) 88.47(8), C(1)-Ru(1)-P(3) 90.25(8), P(2)-Ru(1)-P(3) 178.38(3), C(1)-Ru(1)-P(4) 97.10(8), P(2)-Ru(1)-P(4) 97.75(3), P(3)-Ru(1)-P(4) 81.42(3), C(1)-Ru(1)-P(1) 81.91(8), P(2)-Ru(1)-P(1) 82.13(3), P(3)-Ru(1)-P(1) 98.68(3), P(4)-Ru(1)-P(1) 179.00(2), C(1)-Ru(1)-Cl(1) 179.22(7), P(2)-Ru(1)-Cl(1) 92.27(3), P(3)-Ru(1)-Cl(1) 89.01(3), P(4)-Ru(1)-Cl(1) 82.56(3), P(1)-Ru(1)-

Cl(1) 98.44(3).

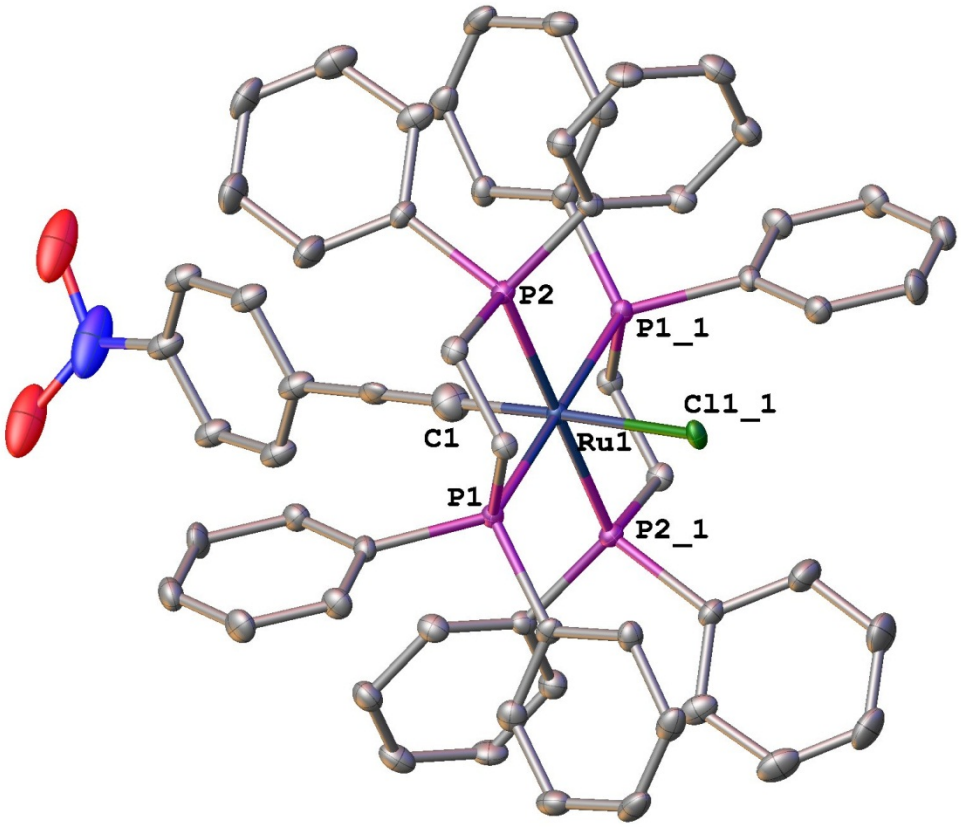


Figure S4. ORTEP plot and atom numbering scheme for *trans*-[Ru(C≡C$C_6H_4$-4-$NO_2$)Cl(dppe)$_2$] **(2a)**, with thermal ellipsoids set at the 30% probability level. Hydrogen atoms and the disordered components of the chloride and 4-nitrophenylethynyl ligands are omitted for clarity. Selected bond lengths (Å) and angles (°) for **2a**: Ru(1)-C(1) 1.87(3), Ru(1)-P(2) 2.3623(17), Ru(1)-P(1) 2.3708(17), Ru(1)-Cl(1)_1 2.398(4), C(1)-Ru(1)-P(2) 93.5(8), C(1)-Ru(1)-P(1) 99.8(8), P(2)-Ru(1)-P(1) 82.75(6), C(1)-Ru(1)-Cl(1)_1 176.9(8), P(2)-Ru(1)-Cl(1)_1 89.50(11), P(1)-Ru(1)-Cl(1)_1 80.40(10). Symmetry operation used to generate equivalent atoms: _1 -x+1,-y+1,-z+1.

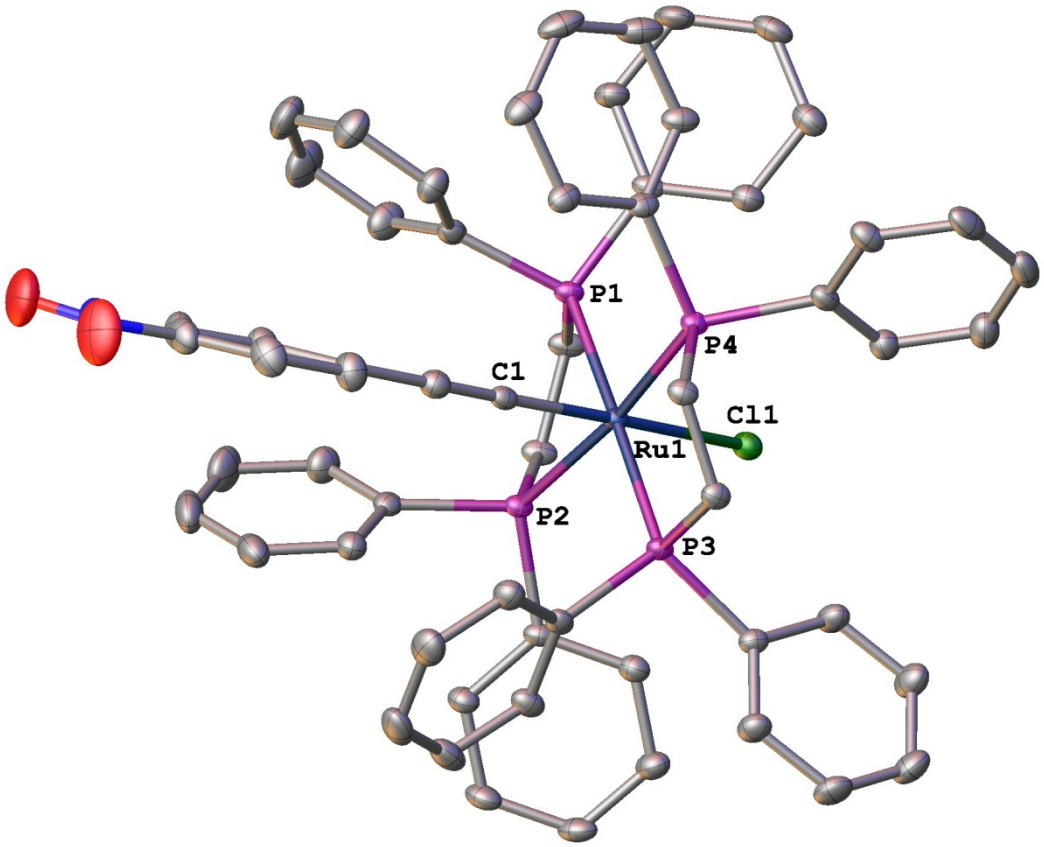


Figure S5. ORTEP plot and atom numbering scheme for *trans*-[Ru(C≡C$C_6H_4$-4-$NO_2$)Cl(dppe)$_2$] **(2b)**, with thermal ellipsoids set at the 30% probability level. Hydrogen atoms and the lattice hexane molecule are omitted for clarity. Selected bond lengths (Å) and angles (°) for **2b**: Ru(1)-C(1) 1.9726(19), Ru(1)-P(2) 2.3503(8), Ru(1)-P(1) 2.3596(7), Ru(1)-P(4) 2.3793(8), Ru(1)-P(3) 2.3896(7), Ru(1)-Cl(1) 2.5351(8), C(1)-Ru(1)-P(2) 90.82(6), C(1)-Ru(1)-P(1) 92.54(6), P(2)-Ru(1)-P(1) 80.30(3), C(1)-Ru(1)-P(4) 81.92(6), P(2)-Ru(1)-P(4) 172.473(17), P(1)-Ru(1)-P(4) 97.94(3), C(1)-Ru(1)-P(3) 86.93(6), P(2)-Ru(1)-P(3) 98.61(4), P(1)-Ru(1)-P(3) 178.782(17), P(4)-Ru(1)-P(3) 83.07(3), C(1)-Ru(1)-Cl(1) 174.05(5), P(2)-Ru(1)-Cl(1) 84.08(3), P(1)-Ru(1)-Cl(1) 83.59(3), P(4)-Ru(1)-Cl(1) 103.06(3), P(3)-Ru(1)-Cl(1) 96.85(3).

**Density Functional Theory.** For the crystals, plane wave/pseudopotential calculations were carried out under 3D periodic boundary conditions with the program Abinit.[12] The PBE functional[13] was used, both in its pure form and in conjunction with Gimme's DFT-D2 dispersion corrections.[14] The pseudopotentials were of Trouiller-Martins type in which the electrons of the next lowest noble gas configuration were frozen. The plane wave cutoff was 1500 eV and a 2×1×1 k-point grid was used for the unit cell of **1**. Nitro groups were necessarily ordered.

The lattice parameters of the ordered crystal of **1** were $a$ = 10.1619, $b$ = 13.4801, $c$ = 14.2681 Å, $\alpha$ = 115.91, $\beta$ = 99.19, $\gamma$ = 103.06°, $V$ = 1636.3 Å$^3$ when relaxed to minimise the PBE energy, a significant cell volume overestimation compared to the experimental results. With DFT-D2 corrections the lattice parameters were $a$ = 9.1163, $b$ = 12.8129, $c$ = 13.2230 Å, $\alpha$ = 117.63, $\beta$ = 93.91, $\gamma$ = 103.70°, $V$ = 1300.7 Å$^3$, smaller than but considerably closer to the experimental unit cell. The differences in the calculated unit cells were almost exclusively intermolecular. For each of the PBE and DFT-D2 relaxations, the final positions for the heavy atoms within individual *trans*-[Ru(C≡C$C_6H_4$-4-$NO_2$)(C≡CPh)(dppe)$_2$] molecules, relative to the Ru atom, were shifted by at most 0.28 Å from those refined from the X-ray data. In both cases most of the larger displacements were associated with a small change in the orientation of a phenyl ring in each dppe ligand. Calculations on 2×1×1 and 1×2×1 supercells of **1** show a negligible difference in energy on swapping alternate nitro groups, consistent with global nitro group disorder. PBE calculations on **2** and **3** performed similarly to those on **1**, with atomic positions being well described but with the poor treatment of dispersion inherent to DFT calculations leading to an expanded unit cell.

For the dipole moments, molecular calculations were performed with the ADF program.[15] Single molecules were taken at the geometries optimized in the crystal calculations. A triple-zeta polarisation basis set.[16] Polarisability was calculated within the TDDFT response theory formalism.[17] The dielectric effect of the surrounding crystal was modelled within the COSMO model.[18]

**Piezoresponse force microscopy (PFM).** Crystals of the ruthenium complexes were washed with *n*-hexane, and then dispersed on a metal plate coated with a thin layer of silver paste to prevent the microcrystals from inadvertently moving. PFM investigations were carried out under ambient conditions using a commercial atomic force microscope (Cypher ES, Asylum Research). Pt-coated Si cantilevers (AC240TM, Olympus) were used for all measurements. In particular, the same cantilever was used for DART-SSPFM of PIN-PMN-PT and **1**. For DART-SSPFM, the presented amplitude-bias and phase-bias loops are an average of two loops. Amplitude-bias loops were shifted to zero the first point. Phase-bias loops were adjusted such that the minimum phase was 0˚. Band excitation switching spectroscopy piezoresponse force microscopy (BE-SSPFM)[19] was realized with a NI PXI-5412 arbitrary waveform generator and a PXIe-5122 digitizer/oscilloscope module. The hardware control and data analysis routines were implemented in a Labview/Igor Pro environment.[20]

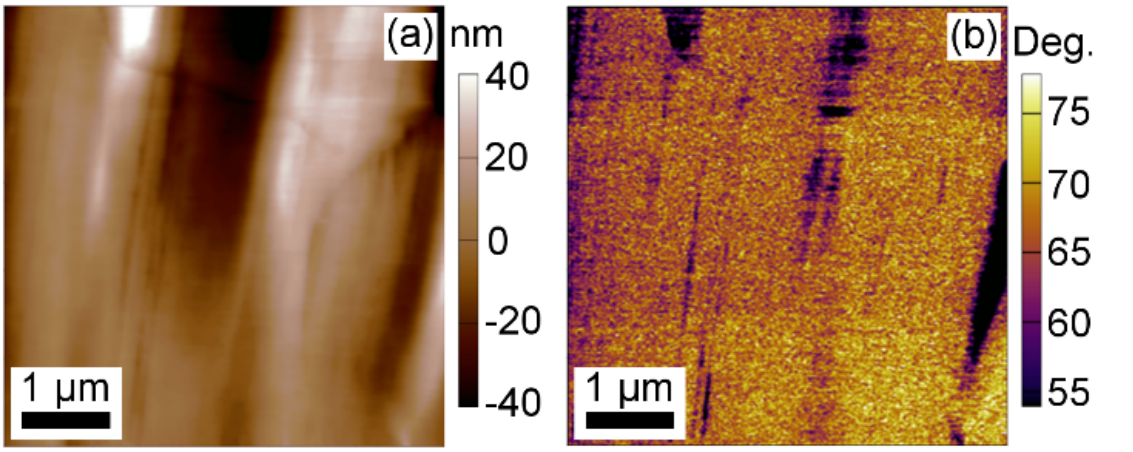


Figure S6. (a) Surface morphology and (b) corresponding PFM phase image of **1**.

## REFERENCES


1. D. Touchard, P. Haquette, S. Guesmi, L. LePichon, A. Daridor, L. Toupet and P. H. Dixneuf, *Organometallics*, 1997, **16**, 3640-3648.
2. M. Morshedi, P. V. Simpson, B. Babgi, K. A. Green, M. S. Jennaway, M. P. Cifuentes and M. G. Humphrey, *Inorg. Synth.*, submitted for publication 14/2/12, paper no IS 37 09.
3. S. Takahashi, Y. Kuroyama, K. Sonogashira and N. Hagihara, *Synthesis*, 1980, 627-630.

4. M. Younus, N. J. Long, P. R. Raithby, J. Lewis, N. A. Page, A. J. P. White, D. J. Williams, M. C. B. Colbert, A. J. Hodge, M. S. Khan and D. G. Parker, *J. Organomet. Chem.*, 1999, **578**, 198-209.
5. Z. Atherton, C. W. Faulkner, S. L. Ingham, A. K. Kakkar, M. S. Khan, J. Lewis, N. J. Long and P. R. Raithby, *J. Organomet. Chem.*, 1993, **462**, 265-270.
6. Z. Otwinowski and W. Minor, *Method. Enzymol.*, 1997, **276**, 307-326.
7. R. H. Blessing, *Acta Crystallogr., Sect. A: Found. Crystallogr.*, 1995, **51**, 33-38.
8. G. M. Sheldrick, *Acta Crystallogr., Sect. A: Found. Crystallogr.*, 2008, **64**, 112-122.
9. O. V. Dolomanov, L. J. Bourhis, R. J. Gildea, J. A. K. Howard and H. Puschmann, *J. Appl. Crystallogr.*, 2009, **42**, 339-341.
10. A. M. McDonagh, M. P. Cifuentes, I. R. Whittall, M. G. Humphrey, M. Samoc, B. LutherDavies and D. C. R. Hockless, *J. Organomet. Chem.*, 1996, **526**, 99-103.
11. P. Vandersluis and A. L. Spek, *Acta Crystallogr., Sect. A: Found. Crystallogr.*, 1990, **46**, 194-201.
12. F. Bottin, S. Leroux, A. Knyazev and G. Zerah, *Comp. Mater. Sci.*, 2008, **42**, 329-336.
13. J. P. Perdew, K. Burke and M. Ernzerhof, *Phys. Rev. Lett.*, 1996, **77**, 3865-3868.
14. S. Grimme, *J. Comput. Chem.*, 2006, **27**, 1787-1799.
15. G. te Velde, F. M. Bickelhaupt, E. J. Baerends, C. F. Guerra, S. J. A. Van Gisbergen, J. G. Snijders and T. Ziegler, *J. Comput. Chem.*, 2001, **22**, 931-967.
16. E. Van Lenthe and E. J. Baerends, *J. Comput. Chem.*, 2003, **24**, 1142-1156.
17. S. J. A. Vangisbergen, J. G. Snijders and E. J. Baerends, *J. Chem. Phys.*, 1995, **103**, 9347-9354.
18. C. C. Pye and T. Ziegler, *Theor. Chem. Acc.*, 1999, **101**, 396-408.
19. S. Jesse, S. V. Kalinin, R. Proksch, A. P. Baddorf and B. J. Rodriguez, *Nanotechnology*, 2007, **18**, 435503.
20. Q. Li, Y. Liu, D. Y. Wang, R. L. Withers, Z. R. Li, H. S. Luo and Z. Xu, *Appl. Phys. Lett.*, 2012, **101**, 242906.